

Ice nucleation and dehydration in the Tropical Tropopause Layer

Eric J. Jensen^{a,1}, Glenn Diskin^b, R. Paul Lawson^c, Sara Lance^c, T. Paul Bui^a, Dennis Hlavka^d, Matthew McGill^e, Leonhard Pfister^a, Owen B. Toon^f, and Rushan Gao^g

^aNational Aeronautics and Space Administration (NASA) Ames Research Center, Moffett Field, CA 94035; ^bNASA Langley Research Center, Hampton, VA 23681; ^cSPEC, Inc., Boulder, CO 80301; ^dScience Systems and Applications, Inc., Lanham, MD 20706; ^eNASA Goddard Space Flight Center, Greenbelt, MD 20771; ^fDepartment of Atmospheric and Oceanic Sciences and Laboratory for Atmospheric and Space Physics, University of Colorado at Boulder, Boulder, CO 80302; and ^gChemical Sciences Division, Earth System Research Laboratory, National Oceanic and Atmospheric Administration, Boulder, CO 80305

Edited by Mark H. Thiemens, University of California at San Diego, La Jolla, CA, and approved December 21, 2012 (received for review October 2, 2012)

Optically thin cirrus near the tropical tropopause regulate the humidity of air entering the stratosphere, which in turn has a strong influence on the Earth's radiation budget and climate. Recent high-altitude, unmanned aircraft measurements provide evidence for two distinct classes of cirrus formed in the tropical tropopause region: (i) vertically extensive cirrus with low ice number concentrations, low extinctions, and large supersaturations (up to ~70%) with respect to ice; and (ii) vertically thin cirrus layers with much higher ice concentrations that effectively deplete the vapor in excess of saturation. The persistent supersaturation in the former class of cirrus is consistent with the long time-scales (several hours or longer) for quenching of vapor in excess of saturation given the low ice concentrations and cold tropical tropopause temperatures. The low-concentration clouds are likely formed on a background population of insoluble particles with concentrations less than 100 L⁻¹ (often less than 20 L⁻¹), whereas the high ice concentration layers (with concentrations up to 10,000 L⁻¹) can only be produced by homogeneous freezing of an abundant population of aqueous aerosols. These measurements, along with past high-altitude aircraft measurements, indicate that the low-concentration cirrus occur frequently in the tropical tropopause region, whereas the high-concentration cirrus occur infrequently. The predominance of the low-concentration clouds means cirrus near the tropical tropopause may typically allow entry of air into the stratosphere with as much as ~1.7 times the ice saturation mixing ratio.

ATTREX | ice nuclei

Although the stratosphere is extremely dry compared with the troposphere, stratospheric humidity plays crucial roles in both atmospheric chemistry and climate. As the primary source of hydroxyl (OH) radicals, H₂O plays an important role in the regulation of stratospheric ozone. Small changes in stratospheric humidity can have significant influence on the Earth's radiation budget and climate (1, 2). Model simulations show that increases in stratospheric humidity enhance the rate of ozone destruction, cool the lower stratosphere, and warm the surface (3, 4).

Air enters the stratospheric overworld (above 380 K potential temperature) almost exclusively via ascent across the tropical tropopause. This fact has motivated interest in understanding processes occurring in the transition layer between the tropical troposphere and stratosphere, a region of the atmosphere referred to as the Tropical Tropopause Layer (TTL). Physical processes occurring in this layer set the boundary condition for the composition and humidity of the stratosphere. It is well established that the aridity of the stratosphere is associated with “freeze-drying” of air as it passes through the cold TTL (5, 6). Deposition growth of ice crystals in optically thin, laminar TTL cirrus depletes vapor in excess of saturation, and the ice crystals sediment relative to the slowly ascending air. The common occurrence of these thin, often subvisible, cirrus in the uppermost tropical troposphere is consistent with this freeze-drying hypothesis. The annual cycle and interannual variability of stratospheric humidity are well correlated

with tropical tropopause temperature variability (7). Despite this general understanding, the details of the regulation of stratospheric humidity, including the role of deep convection, transport pathways, and cloud microphysical processes, have been subjects of considerable debate (8–10).

Before the measurements described here, available observational evidence indicated that the ice concentrations in cirrus that formed in the TTL were surprisingly low. High-altitude aircraft sampling in various tropical locations indicated ice concentrations almost exclusively less than 100 L⁻¹ (11–16). This result is in conflict with theoretical expectations. Given the ubiquitous presence of mesoscale-wave temperature fluctuations in the TTL, the conventional theory of ice nucleation via homogeneous freezing of aqueous aerosols predicts much higher ice concentrations (13, 15, 17). Ice concentrations of approximately 4,000 L⁻¹ in midlatitude wave clouds with strong updrafts have been shown to be consistent with homogeneous freezing theory (18). Various possible explanations for the low ice concentrations have been put forward. Recent laboratory experiments show that if aqueous aerosols contain high-molecular-weight organics, then a glass transition will occur at low temperatures (19, 20). The viscosity in the aerosols then becomes extremely high, preventing the growth of an ice germ. Alternatively, TTL ice production may be dominated by heterogeneous nucleation, in which case the concentration of ice crystals could be limited by the abundance of effective ice nuclei (IN) because growth of the ice crystals nucleated on the IN could quench the supersaturation in cooling air parcels such that further nucleation does not occur (21). Candidate sources of IN include dust particles, dry ammonium sulfate particles, and glassy organic-containing aerosols (15, 22). Measurements of ice crystal residuals indicate no preference for particular aerosol compositions acting as IN (23). However, the limited information about TTL aerosol composition and physical state precludes any clear identification of the IN composition. Distinguishing the modes of ice nucleation in TTL cirrus has been hampered by uncertainties in water vapor measurements under the dry TTL conditions as well as persistent discrepancies between water vapor measurements made with different instruments (24, 25).

Methods

The importance of TTL physical processes and their poor representation in global models motivated the NASA Airborne Tropical Tropopause Experiment (ATTREX). A series of airborne campaigns is being conducted using the recently acquired NASA Global Hawk Unmanned Aircraft System. The ceiling (65,000 feet) and long duration (30 h) of the Global Hawk make it an ideal platform for sampling the TTL. The ATTREX Global Hawk payload includes

Author contributions: E.J.J. designed research; E.J.J., G.D., R.P.L., S.L., T.P.B., D.H., M.M., L.P., O.B.T., and R.G. performed research; E.J.J., G.D., R.P.L., and S.L. analyzed data; and E.J.J. wrote the paper.

The authors declare no conflict of interest.

This article is a PNAS Direct Submission.

¹To whom correspondence should be addressed. E-mail: eric.j.jensen@nasa.gov.

instrumentation for measuring cloud properties, water vapor, meteorological conditions, radiative fluxes, chemical species, and numerous tracers. The first ATTREX flights occurred during the fall of 2011.

Here we focus on measurements of cirrus and relative humidity collected during Global Hawk ascents and descents through the TTL. Water vapor concentration is measured with the diode laser hygrometer (DLH), which has flown on aircraft for 15 y. DLH uses a near-infrared external open-path diode laser spectrometer to provide precise measurements of water vapor concentration (precision of 50 ppbv for 20-Hz measurements) (26). The estimated accuracy of the DLH water vapor measurements is 10% in the 1–10 ppmv range. We note that past comparisons between airborne water vapor measurements (not including DLH in its ATTREX configuration) under such dry conditions have indicated discrepancies between different instruments that are considerably larger than 10% (27). These discrepancies remain unresolved at this time. As discussed below, the ATTREX DLH measurements indicating ice saturation ratio near unity in clouds with very high ice concentrations provide some confidence in the accuracy of the measurements.

Cloud microphysical properties are measured with the Fast Cloud Droplet Probe (FCDP). FCDP is a spectrometer that measures the forward scattered laser light from individual cloud particles and infers the size of the cloud particles from 1 to 50 μm diameter (28). The instrument was designed for measurements of water clouds and assumes Mie scattering to retrieve particle size. Because of uncertainties associated with sizing nonspherical ice particles, we rely mainly on FCDP particle concentration measurements and use particle size measurements cautiously. We assume that all particles detected by the FCDP are ice crystals because the presence of appreciable concentrations of supermicron aerosol particles in the TTL is unlikely. This assumption is supported by the lack of FCDP detection of particles in subsaturated air. Temperature, pressure, and winds are measured with the Meteorological Measurement System (MMS). MMS provides calibrated in situ measurements of static pressure, static temperature, and 3D winds using an air motion sensing system and ring laser Inertial Navigation System (29).

Calibrated in situ static pressure and temperature are achievable as the result of the wind measurements. Ozone concentration is measured with a dual-beam UV absorption photometer (30). We also use the remote-sensing extinction measurements from the Cloud Physics Lidar (CPL) (31). CPL measures backscattered radiation at 355, 532, and 1,064 nm. Extinction is determined on the basis of an estimate of the backscatter-to-extinction ratio.

Results and Discussion

On the flight of November 5–6, 2011, the Global Hawk descended and ascended through the TTL (between approximately 15.5 and 17 km) several times in the northern part of an anomalously cold tropopause region in the eastern Pacific (at approximately 125°W and 11°N). The TTL thermal structure is highly variable, both horizontally and vertically, indicative of considerable wave activity (Fig. 1). Much of the tropopause region is highly supersaturated with respect to ice, with ice saturation ratios (S_i) as high as ~ 1.7 . The existence of large ice supersaturations at low temperatures is plausible given the numerous laboratory experiments showing that homogenous freezing of aqueous aerosols does not occur until S_i exceeds values of approximately 1.6–1.7 at low temperatures (32).

The FCDP measurements indicate that ice crystals were present through the depth of most of the TTL supersaturated layers (gray shading in Fig. 1), with ice concentrations generally well below 100 L^{-1} . Embedded in some of these low ice concentration clouds are narrow layers with much higher ice concentrations (black bars in Fig. 1) that are typically on the order of 1,000 L^{-1} and as high as 10,000 L^{-1} . Associated with each of these high ice concentration layers are sharp decreases in water vapor concentration and corresponding decreases in ice saturation to near unity. The water

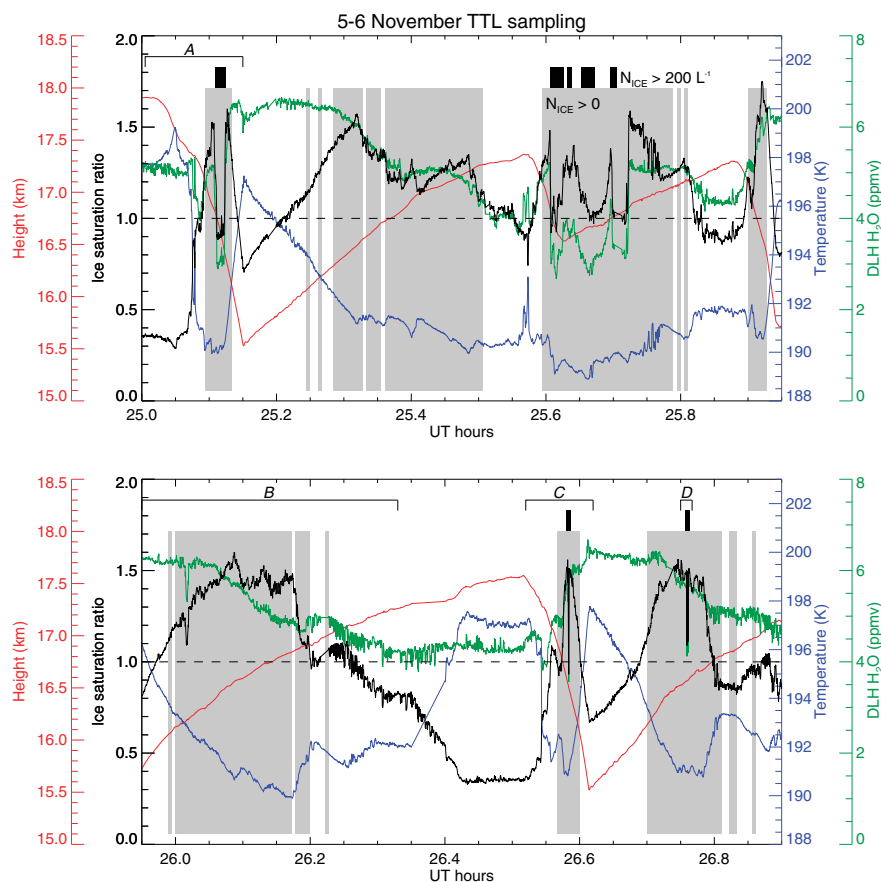


Fig. 1. Time series of in situ measurements during ascents and descents through the TTL. Height (black), temperature (blue), water vapor mixing ratio (green), and ice saturation ratio (red). Gray shading indicates time periods when ice was detected, and black bars indicate times when high ice concentrations ($>200 \text{ L}^{-1}$) were present. The time ranges indicated by A–D correspond to the vertical profiles shown in Fig. 3.

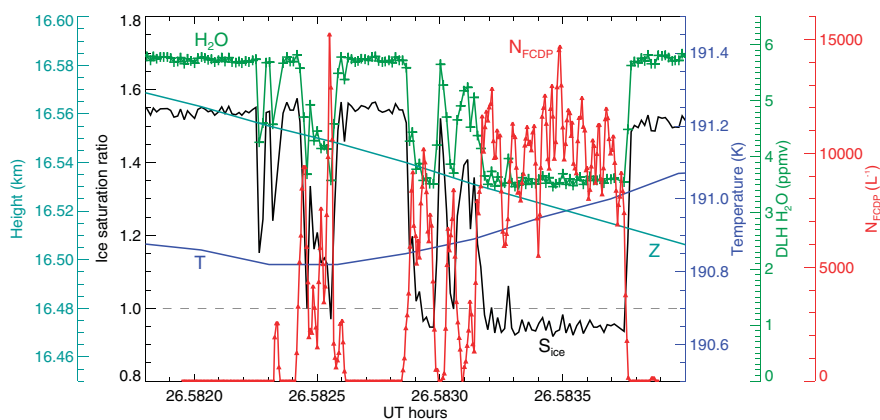


Fig. 2. Expansion of the time period labeled C in Fig. 1. Within the cloud layer with very high ice concentration ($N_{\text{FCDP}} \approx 2,000\text{--}10,000\text{ L}^{-1}$), the water vapor concentration is nearly constant, and the ice saturation ratio is held near unity. Twenty-hertz water vapor and cloud particle concentration data are used here.

vapor concentration decreases in these cloud layers by as much as a factor of 2, from approximately 6 ppmv to 3 ppmv. The high-concentration clouds and vapor layers are as narrow as 2 m in vertical extent, indicating very localized ice nucleation.

Because the time scale for removal of vapor in excess of saturation in a cloud with ice concentrations exceeding $1,000\text{ L}^{-1}$ is on the order of 10 min or less, the ice saturation is expected to be held near unity. Maintenance of a 10% supersaturation/subsaturation in this cloud layer would require a vertical wind speed of a few 10 s^{-1} . Such updraft/downdraft speeds are plausible in high-frequency gravity waves, but larger vertical wind speeds occur infrequently (17). During the 30-s pass through the cloud with exceedingly high ice concentrations ($2,000\text{--}10,000\text{ L}^{-1}$), the 20-Hz DLH water vapor concentration indicates little variability, and the ice saturation (indicated by the DLH and MMS water vapor and temperature measurements) is constant near unity (Fig. 2). Note also that the ice saturation ratio indicated by DLH is near unity on multiple passes through the high-concentration clouds. Because the vapor pressure over ice is well known at these temperatures, it is likely that the DLH measurements are accurate to within 10%.

The vertical structure of cloud properties and relative humidity can be seen more clearly by examining individual profiles through the TTL (Fig. 3). Here we clearly see two distinct classes of TTL cirrus. Fig. 3B shows an example of a low ice concentration cloud that nearly spans the supersaturated layer. Large ice supersaturations are persistent in this layer, consistent with the lack of sufficient numbers of crystals to rapidly deplete vapor in excess of saturation by deposition growth. Embedded in some of these low ice concentration clouds are layers with much higher ice concentrations and all vapor in excess of saturation effectively depleted by crystal growth. Fig. 3A shows an example of a relatively deep layer with high ice concentrations, whereas the profiles shown in Fig. 3C and D show examples of very narrow high-concentration layers. The expanded scale in Fig. 3D shows that two distinct layers were present, with vertical thicknesses of 2 and 4 m. Because the aircraft ascends relatively slowly (approximately 2 m s^{-1}), it is possible that these were two horizontally as well as vertically separated layers. It seems likely that these cloud layers were detected shortly after nucleation occurred, such that growth and sedimentation had not had a chance to increase the cloud depth.

The CPL laser was shut down during ascents and descents, thus we do not have lidar measurements for the specific cloud shown in Figs. 1–3. However, time–height curtains of TTL cirrus extinction from the CPL lidar (Fig. 4) generally indicate cloud structures consistent with the in situ observations. Broad layers with low extinction (blue colors) correspond to the relatively deep layers with low ice concentrations observed in situ. Embedded within these low-extinction clouds are narrow layers with much higher

extinctions, corresponding to the narrow layers with high ice concentrations indicated by the in situ measurements. Below 15 km, the lidar reveals the tops of convective systems.

In all likelihood, the clouds above 15 km were formed in situ within the TTL rather than as a result of detrainment from deep convection. Geostationary satellite imagery and trajectory analysis indicate no deep convection extending to these altitudes within 14 d upstream of the observations. The ozone concentration was approximately 100 ppbv, typical of aged TTL air, and it was the same above, below, and within the cloud layers above 15 km. In contrast, on descents through cirrus recently detrained from deep convection on the November 9 flight, the ozone concentration decreased to much lower values consistent with transport from the clean marine boundary layer.

Homogeneous freezing of aqueous aerosols is the only plausible explanation for the high ice concentration cloud layers. Measurements of heterogeneous IN concentrations almost never indicate values exceeding 100 L^{-1} outside of dense mineral dust layers (33). The high ice concentrations reported here are consistent with theoretical predictions of homogeneous freezing nucleation driven by rapid cooling (34).

The broader, more commonly occurring, low ice concentration clouds likely result from heterogeneous nucleation on a small subset of the total aerosol population. It is important to note that these low ice concentration clouds exist above, below, and in the absence of the high ice concentration layers. If the sparse clouds were only observed below the high ice concentration layers, then a plausible hypothesis would be that diffusion and/or sedimentation transported a small fraction of the ice crystals in the high-concentration layer into the supersaturated air below. Once in the lower layer, the ice could rapidly grow and sediment, producing a deeper layer with low ice concentrations (35). Instead, the presence of the sparse layers above and below the high ice concentration layers suggests that supersaturations never reached high enough values to nucleate ice homogeneously except in the high-concentration layers, whereas heterogeneous nucleation occurred in the deeper layers.

The high ice concentration layers are not generally associated with prominent temperature minima in the vertical profiles (nor with vertical wind shear or abrupt changes in ozone). However, as discussed above, the horizontal and vertical temperature variability indicates significant wave activity, and it is possible that colder temperatures upstream of the measurements led to higher supersaturations and homogeneous freezing that produced the high ice concentration layers. It is somewhat surprising that homogenous freezing is not more common, given the prevalence of high supersaturations apparent in Figs. 1 and 2. It is also surprising that high ice concentration layers have not been observed in any of the

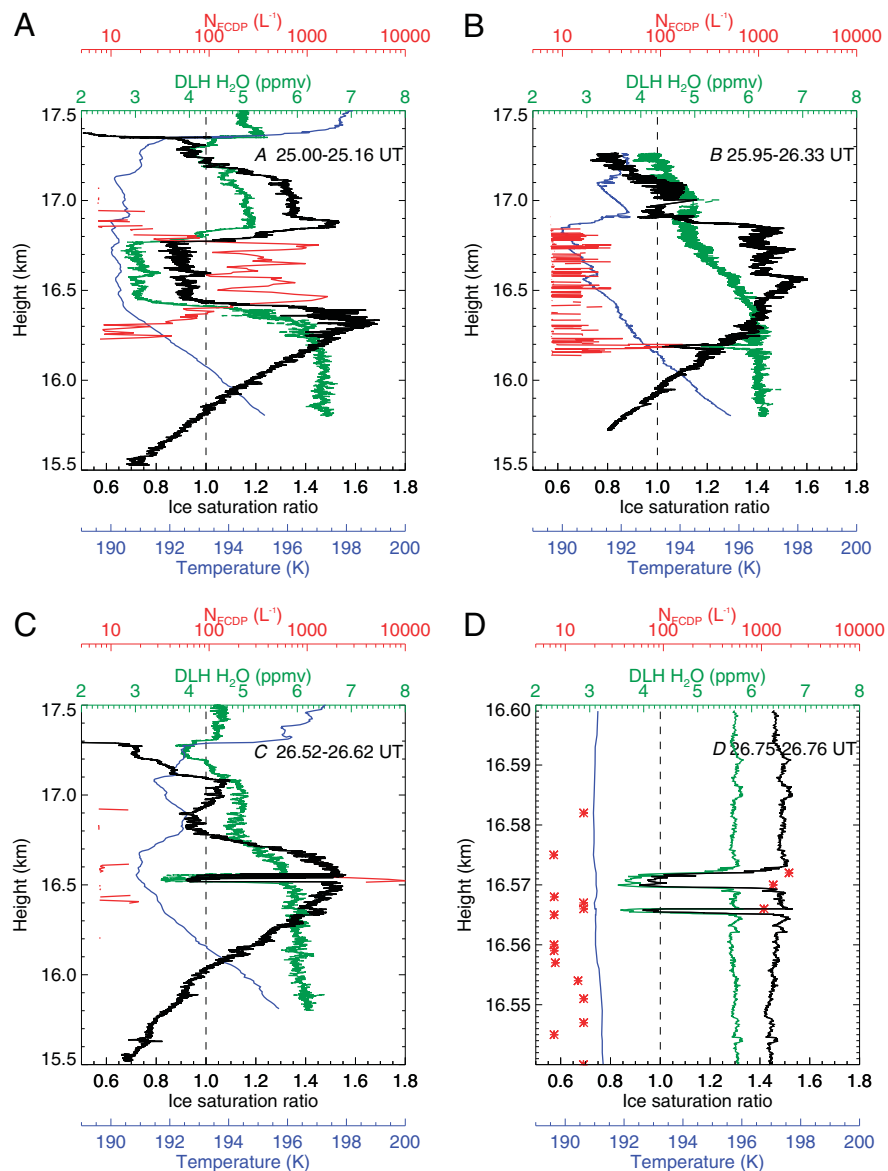


Fig. 3. Vertical profiles of temperature (blue), water vapor mixing ratio (green), ice saturation ratio (black), and ice concentration (red) for individual profiles described in Fig. 1. (A, C, and D) Examples of cloud layers with high ice concentration, within which vapor in excess of ice saturation is depleted by ice growth. (B) Example of a deep layer with low ice concentration and persistent high ice supersaturation.

previous in situ high-altitude aircraft campaigns that sampled TTL cirrus (11–16). As discussed above, it is possible that the typical TTL aerosol composition or physical state prevents homogeneous freezing, and the high ice concentration layers reported here could perhaps have formed in isolated lamina with aqueous aerosols that could freeze. Small-scale waves may also cause localized nucleation by driving the temperature below the threshold for homogeneous freezing. Given the lack of aerosol physical state or upwind gravity-wave measurements, we do not have a clear explanation for the fact that homogeneous freezing seems to occur in isolated narrow layers.

In terms of impacts on climate and stratospheric chemistry, a critical issue is how effectively these clouds dehydrate air ascending across the tropical tropopause. The measurements presented here indicate that growth of ice crystals in the high-concentration clouds effectively depletes vapor in excess of saturation; however, this alone does not necessarily imply that irreversible dehydration has occurred. If we assume that the ice water content is equal to the apparent depletion in water vapor (approximately 2.5 ppmv at a

temperature and pressure of 191 K and 102 hPa), then we can estimate the ice crystal size from the measured concentration. An ice concentration of 1,000 L⁻¹ would imply an equivalent-sphere diameter of 8.5 μm, with a corresponding fallspeed of approximately 0.3 cm s⁻¹. We can roughly estimate the cloud lifetime from the thermal structure and wind speed in the region where the cloud was sampled. Assuming the cloud will only exist in the region with temperatures ~1–2 K below the upstream and downstream temperatures, the ~15 m s⁻¹ wind speed gives a cloud lifetime of several hours. In this time, the small ice crystals in the high-concentration layers would fall only approximately 80 m. The depths of the high-concentration cloud layers ranged from approximately 2 to 500 m. Hence, these clouds likely will not irreversibly dehydrate the deeper layers, and they will typically leave behind narrow dehydrated layers.

As shown in Fig. 3, supersaturation persists in the low-concentration TTL cirrus, with ice saturation ratios up to near the threshold for homogeneous freezing of aqueous aerosols ($s_{ice} \approx 1.7$). The FCDP measurements indicate diameters in the

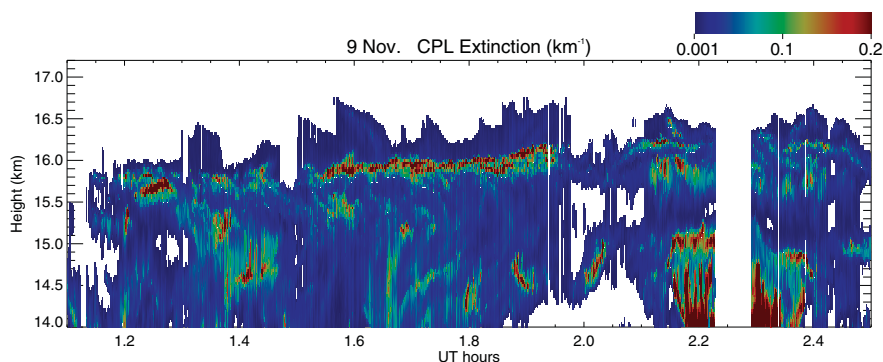


Fig. 4. Extinction (km^{-1}) vs. time and height indicated by the nadir-looking CPL. Flight segment on November 9 is shown. Narrow layers with high extinction are embedded in broader layers with low extinction.

low-concentration cirrus on the order of $30\text{--}50\ \mu\text{m}$ (and possibly larger, because $50\ \mu\text{m}$ is the upper sizing limit of the FCDP). Given a cloud lifetime of several hours, these ice crystals would fall a few km through saturated air, effectively removing the condensed water from the uppermost TTL. However, the measurements indicate that the low-concentration cirrus do not effectively remove vapor in excess of saturation. The time scale for quenching of supersaturation in the low ice concentration clouds is on the order of several hours, and even relatively slow cooling can maintain substantial supersaturation (13). Hence, these clouds will not prevent highly supersaturated air from ascending across the tropical tropopause.

The results presented here have implications for assumptions made about TTL dehydration in models. Lagrangian trajectory analysis is commonly used to relate annual and interannual variability in stratospheric humidity to transport pathways and TTL temperatures (36–38). These analyses generally assume that any vapor in excess of ice saturation along the trajectories is completely removed from the TTL. However, we find that large supersaturations can persist in the low ice concentration cirrus. The ATTREX measurements, as well as measurements from several previous high-altitude aircraft campaigns, indicate that these low-concentration cirrus are prevalent throughout the TTL (11–16). The high ice concentration cirrus reported here seem to occur much less frequently. The implication is that air can commonly ascend across the cold tropical tropopause with as much as ~ 1.7 times the minimum saturation mixing ratio (i.e., up to the threshold for homogeneous freezing). Even the high-concentration layers will only irreversibly dehydrate very narrow layers, given the necessarily small ice crystals in these clouds. These conclusions are consistent with the fact that the trajectory analyses assuming all vapor in excess of saturation is removed generally produce

stratospheric water vapor concentrations lower than indicated by satellite measurements (38).

The measurements reported here were made in November, and the water vapor concentration near the tropopause was still relatively high (~ 5 ppmv), perhaps indicating persistent moist air from the wet summertime phase of the annual tropical tropopause temperature variation. The dehydration events observed on the Global Hawk ascents/descents through the TTL show sharp, localized decreases in water vapor concentration associated with cold anomalies occurring at the beginning of the wintertime season. The dehydration events no doubt increase in frequency as time progresses into the coldest months (December–January–February). Satellite measurements with coarse vertical and horizontal resolution indicate a gradual decrease in tropical tropopause water vapor concentrations through the winter (39). The in situ aircraft measurements show that dehydration events are actually very localized and occur in narrow vertical layers, with large decreases in water vapor concentration.

ATTREX includes three more flight series over the next 2 y, and we hope to gather information about the relative occurrence frequency of the two classes of TTL cirrus identified here. In particular, we plan to investigate the dependence of TTL cirrus microphysics and dehydration on season, geographic location, and temperature. Modeling studies that incorporate the observed cloud microphysical properties (and effects on water vapor) are required to evaluate the impact of these findings on the global radiation budget and stratospheric humidity.

ACKNOWLEDGMENTS. We thank the Dryden Flight Research Center Global Hawk crew and pilots for making these measurements possible. This research was funded by the NASA Airborne Tropical Tropopause Experiment and the NASA Radiation Sciences Program.

- Forster PMDF, Shine KP (2002) Assessing the climate impact of trends in stratospheric water vapor. *Geophys Res Lett* 29:1086.
- Solomon S, et al. (2010) Contributions of stratospheric water vapor to decadal changes in the rate of global warming. *Science* 327(5970):1219–1223.
- Dvorstov VL, Solomon S (2001) Response of the stratospheric temperatures and ozone to past and future increases in stratospheric humidity. *J Geophys Res* 106:7505–7514.
- Shindell DJ (2001) Climate and ozone response to increased stratospheric water vapor. *Geophys Res Lett* 28:1551–1554.
- Brewer AM (1949) Evidence for a world circulation provided by the measurements of helium and water vapor distribution in the stratosphere. *Q J R Meteorol Soc* 75: 351–363.
- Jensen EJ, Toon OB, Pfister L, Selkirk HB (1996) Dehydration of the upper troposphere and lower stratosphere by subvisible cirrus clouds near the tropical tropopause. *Geophys Res Lett* 23:825–828.
- Randel WJ, et al. (2006) Decreases in stratospheric water vapor after 2001: Links to changes in the tropical tropopause and the Brewer-Dobson circulation. *J Geophys Res* 111:D12312.
- Sherwood SC, Dessler AE (2000) On the control of stratospheric humidity. *Geophys Res Lett* 27:2513–2516.
- Jensen EJ, Pfister L (2004) Transport and freeze-drying in the tropical tropopause layer. *J Geophys Res* 109:D02007.
- Dessler AE, Hanisco TF, Fueglistaler S (2007) Effects of convective ice lofting on H_2O and HDO in the tropical tropopause layer. *J Geophys Res* 112:D18309.
- McFarquhar GM, Heymsfield AJ, Spinhirne J, Hart B (2000) Thin and subvisual tropopause tropical cirrus: Observations and radiative impacts. *J Atmos Sci* 57: 1841–1853.
- Lawson RP, et al. (2008) Aircraft measurements of microphysical properties of sub-visible cirrus clouds in the tropical tropopause layer. *Atmos Chem Phys* 8:1609–1620.
- Krämer M, et al. (2009) Ice supersaturations and cirrus cloud crystal numbers. *Atmos Chem Phys* 9:3505–3522.
- Schmitt C, Heymsfield A (2009) The size distribution and mass weighted terminal velocity of low-latitude tropopause cirrus crystal populations. *J Atmos Sci* 65: 982–1003.
- Jensen EJ, et al. (2010) Ice nucleation and cloud microphysical properties in tropical tropopause cirrus. *Atmos Chem Phys* 10:1369–1384.
- Frey W, et al. (2011) In situ measurements of tropical cloud properties in the West African Monsoon: Upper tropospheric ice clouds, Mesoscale Convective System outflow, and subvisual cirrus. *Atmos Chem Phys* 11:5569–5590.

17. Jensen EJ, Pfister L, Bui TP (2012) Physical processes controlling ice concentrations in cold cirrus near the tropical tropopause. *J Geophys Res* 117:D11205.
18. Jensen EJ, et al. (1998) Ice nucleation processes in upper tropospheric wave-clouds observed during SUCCESS. *Geophys Res Lett* 25:1363–1366.
19. Zobrist B, Marcolli C, Penderner DA, Koop T (2008) Do atmospheric aerosols form glasses? *Atmos Chem Phys* 8:5221–5244.
20. Murray BJ (2008) Inhibition of ice crystallization in highly viscous aqueous organic acid droplets. *Atmos Chem Phys* 8:5423–5433.
21. Gensch IV, et al. (2008) Supersaturations, microphysics and nitric acid partitioning in a cold cirrus cloud observed during CR-AVE 2006: An observation-modeling intercomparison study. *Environ Res Lett* 3:1–9.
22. Murray BJ, et al. (2010) Heterogeneous nucleation of ice particles on glassy aerosols under cirrus conditions. *Nat Geosci* 3:233–237.
23. Froyd K, et al. (2010) Aerosols that form subvisible cirrus at the tropical tropopause. *Atmos Chem Phys* 10:209–218.
24. Kley D, Russell JM, III, Phillips C, eds (2000) *SPARC Assessment of Upper Tropospheric and Stratospheric Water Vapor* (World Climate Research Programme, Geneva).
25. Jensen EJ, et al. (2008) Formation of large ($\approx 100 \mu\text{m}$) ice crystals near the tropical tropopause. *Atmos Chem Phys* 8:1621–1633.
26. Podolske JR, Sachse GW, Diskin GS (2003) Calibration and data retrieval algorithms for the NASA Langley/Ames Diode Laser Hygrometer for the NASA Transport and Chemical Evolution Over the Pacific (TRACE-P) mission. *J Geophys Res* 108:8792.
27. Weinstock EM, et al. (2009) Validation of the Harvard Lyman- α in situ water vapor instrument: Implications for the mechanisms that control stratospheric water vapor. *J Geophys Res* 114:D23301.
28. McFarquhar GM, et al. (2007) The importance of small ice crystals to cirrus properties: Observations from the Tropical Warm Pool International Cloud Experiment (TWP-ICE). *Geophys Res Lett* 57:L13803.
29. Scott SG, et al. (1990) The meteorological measurement system on the NASA ER-2 aircraft. *J Atmos Ocean Technol* 7:525–540.
30. Gao RS, et al. (2012) A compact, fast UV photometer for measurement of ozone from research aircraft. *Atmos Meas Tech* 5:2201–2210.
31. McGill MJ, et al. (2002) Cloud physics lidar: Instrument description and initial measurement results. *Appl Opt* 41(18):3725–3734.
32. Koop T, Luo B, Tsias A, Peter T (2000) Water activity as the determinant for homogeneous ice nucleation in aqueous solutions. *Nature* 406(6796):611–614.
33. DeMott PJ, et al. (2003) Measurements of the concentration and composition of nuclei for cirrus formation. *Proc Natl Acad Sci USA* 100(25):14655–14660.
34. Kärcher B, Lohmann U (2002) A parameterization of cirrus cloud formation: Homogeneous freezing of supercooled aerosols. *J Geophys Res* 107:4010.
35. Dhaniyala S, McKinney KA, Wennberg PO (2002) Lee-wave clouds and denitrification of the polar stratosphere. *Geophys Res Lett* 29:1322.
36. Gettelman A, Randel WJ, Wu F, Massie ST (2002) Transport of water vapor in the tropical tropopause layer. *Geophys Res Lett* 29:1009.
37. Fueglistaler S, Bonazzola M, Haynes PH, Peter T (2005) Stratospheric water vapor predicted from the Lagrangian temperature history of air entering the stratosphere in the tropics. *J Geophys Res* 110:D08107.
38. Liu YS, Fueglistaler S, Haynes PH (2010) Advection-condensation paradigm for stratospheric water vapor. *J Geophys Res* 115:D24307.
39. Mote PY, et al. (1996) An atmospheric tape recorder: The imprint of tropical tropopause temperatures on stratospheric water vapor. *J Geophys Res* 101:3989–4006.